

Magnetic domain and magnetic resistance phase transition in strongly correlated electronic material of perovskites junction

Ren R†, Weiren Wang, Xuan Li, Zhongxia Zhao

Department of optics , Xian Jiao Tong University, Xi'an, 710054, China

The junction magnetoresistivity and domain phase transition were studied between ZnO and $\text{La}_{0.4}\text{Gd}_{0.1}\text{Sr}_{0.5}\text{CoO}_3$ thin films grown on LaAlO_3 (100) substrates epitaxially by pulse laser deposit. The ferromagnetic transformation into phase-separated (two phase) state was displayed below $T_c \sim 127$ and has observed that the lattice change discontinuously in the doped cobalt perovskites $\text{La}_{0.4}\text{Gd}_{0.1}\text{Sr}_{0.5}\text{CoO}_3$. The Ginzburg-Landau phase field is introduced to deduce antiferroelectric domain structure in LGSCO thin film. On the basis of the domain structures, the phase boundary of thin film is strongly dependent on the combination of electric-mechanical coupling. The phase transformation into phase separated state occurs below $T_c \sim 127\text{-}128\text{K}$, and have displayed that the lattice constants change discontinuously at the transformation. The positive MR of ZnO/LGSCO heterojunction exhibited the MIT behavior at 0.2 T is 4.86%, at 0.5 T is 6.05% for approximately 140K.

Keywords: magnetic domain, magnetoresistivity, carrier injection, spin-orbit, MIT transition

PACS: 42.87.-d ,75.70.Kw,75.10.Hk, 73.22.2f, 73.61.Wp, 73.63.Rt, 52.38.-r

DOI:10.1063/1.1850192

Author to whom correspondence should be addressed mail: renrnano@126.com

1. INTRODUCTION

Recently, it is found that LaCoO_3 was charge transfer insulator,^{[9],[10]} while $\text{La}_{0.7}\text{Sr}_{0.3}\text{CoO}_3$ was intermediate between charge transfer and Mott insulator and the ferromagnetic ordering and insulate-metal Hubbard-type compounds.^[11] The spin ordering, charge, transition, as well as the colossal magnetoresistance and orbit ordering transition observed at around the CMR phenomenon which make $\text{R}_{1-x}\text{A}_x\text{CoO}_3$ half-filling is strongly coupled with lattice distortion. $\text{ZnO}/\text{La}_{0.4}\text{Gd}_{0.1}\text{Sr}_{0.5}\text{CoO}_3$ heterojunction an interesting Chen explored the electronic transport of candidate for ferromagnetic and ferroelectric $\text{Al}:\text{ZnO}/\text{BiFeO}_3/\text{ITO}$ junction related to electron applications. Especially, CMR effect is strengthened spin-dependent scattering and the interface resistance near the phase separated between the charge ordered^[16] In the DE mechanism, the ferromagnetic phase insulator and the ferromagnetic metal. $\text{R}_{1-x}\text{A}_x\text{CoO}_3$ has a transition was suggested to be introduced by hopping of rhombohedral perovskite structure, lead to altered spin eg electrons between Co^{3+} and Co^{4+} through the oxygen ordering and phase boundary, which is due to Co^{3+} and ions that also result from conductivity in carriers Co^{4+} having spin Co^{3+} $t_{2g}^6e_g^0$, $t_{2g}^5e_g^1$, and $t_{2g}^4e_g^2$ under transport. The heterojunction quantum energy band was various doped concentration and temperature.^[1,2] ZnO modified by spin, orbital ordering, and lattice field to is generally regarded as n-type due to oxygen impurity, exhibit photoinduced resistance and colossal and their carrier concentration is dominated by oxygen magnetoresistance (CMR) effect.^[1,2,4,7] However, the deficiency. So far, many theoretical and experimental phase transition and domain separation mechanism of studies have been carried out on the phase boundary ZnO/LGSCO heterojunction are little explored from the problem. Among them, LSCO, which is ferromagnetic direction of junction CMR effect in the heterostructure but is transferred in to antiferromagnetic charge in the past few years. Furthermore, the insulator (CI) phase below T_{CI} have exhibited $\text{La}_{0.4}\text{Gd}_{0.1}\text{Sr}_{0.5}\text{CoO}_3$ topological evolutions by 2D grain coexistence of FM and CI microdomains.^[6] Phase growth using a continued diffuse interface field are little separation in rare-earth metals of studied. The ferromagnetic and charge properties are hydrogen-concentration have been investigated at attributed to the further understanding of charge ambient temperature and high pressure by x-ray ordering, magnetic order, electric-mechanical coupling, diffraction changed in structural, electronic, and spin-orbital coupling, optical field and lattice structure. magnetic properties.^[7] Goodenough reported the The domain wall orientations structure and structural and magnetic properties of the metallic spin-orbital coupling strongly influence the ferroelectric double-perovskite system, and suggested that and antiferromagnetic properties of ferromagnetic long-range ordered domains are coupled $\text{ZnO}/\text{La}_{0.4}\text{Gd}_{0.1}\text{Sr}_{0.5}\text{CoO}_3$. The LGSCO material was antiferromagnetically across antiphase boundaries, accompanied from ferromagnetic to antiferromagnetic random disorder within domains may be transition, which is called double exchanged P doping. small.^{[20],[27]} Yacaman et al. investigate the self-assembly $\text{La}_{0.4}\text{Gd}_{0.1}\text{Sr}_{0.5}\text{CoO}_3$ from ferromagnetic to of this material through controlling the material antiferromagnetic ordering was accompanied by a Co^{3+} / structure and chemical order and found that bimetallic Co^{4+} charge orbit ordering. The mechanics and electric core/shell has the structure of faced centered cubic coupling of $\text{ZnO}/\text{La}_{0.4}\text{Gd}_{0.1}\text{Sr}_{0.5}\text{CoO}_3$ thin films strongly octahedron.^{[19],[22]} The FM metallic state and the influence domain structure and domain wall. Domain charge/orbital ordered insulator Cr-doped walls can produce pinning sites that reduce remnant $\text{Nd}_{0.5}\text{Ca}_{0.5}\text{MnO}_3$ have ferromagnetic (FM) polarization, as well as domain structure plays a role in microdomains in the phase-separated state and FM ferroelectric and ferromagnetic order. microdomains.^[9] Rivadulla studied perovskite oxide^[18] In this work, we present the structural analysis spin glass phase separation behavior. elucidated the phase separated state in the

heterojunction of cobalt perovskites $\text{La}_{0.4}\text{Gd}_{0.1}\text{Sr}_{0.5}\text{CoO}_3$ and ZnO films fabricated by pulse laser deposition surface morphology $\text{ZnO}/\text{La}_{0.4}\text{Gd}_{0.1}\text{Sr}_{0.5}\text{CoO}_3/\text{LAO}$. consist of ZnO and $\text{La}_{0.4}\text{Gd}_{0.1}\text{Sr}_{0.5}\text{CoO}_3$ grown on The bright region was hard phase, and the dark region LaAlO substrate. The IMT effect is enhanced near the was soft phase. The FIG. show the surface roughness for phase boundary between the ferromagnetic metallic(FM) $\text{ZnO}/\text{La}_{0.4}\text{Gd}_{0.1}\text{Sr}_{0.5}\text{CoO}_3/\text{Si}$ was 2nm and the surface and the charge-ordered insulating phase, where the quality is very well.AFM results were presented for phase separation effect is also enhanced. The $\text{ZnO}/\text{La}_{0.4}\text{Gd}_{0.1}\text{Sr}_{0.5}\text{CoO}_3/\text{LaAlO}$ and $\text{ZnO}/\text{La}_{0.4}\text{Gd}_{0.1}\text{Sr}_{0.5}\text{CoO}_3/\text{ZnO}$ junction exhibited excellent $\text{La}_{0.4}\text{Gd}_{0.1}\text{Sr}_{0.5}\text{CoO}_3/\text{Si}$,respectively.

rectifying behavior and MR properties over the $\text{ZnO}/\text{La}_{0.4}\text{Gd}_{0.1}\text{Sr}_{0.5}\text{CoO}_3$ film displayed very smooth temperature range of 80-300K. The Ginzburg-Landau surface with uniform grain size of 31nm and the phase field is used to evolution antiferroelectric domain interface roughness of $\text{ZnO}/\text{La}_{0.4}\text{Gd}_{0.1}\text{Sr}_{0.5}\text{CoO}_3$ was structure LGSCO thin film. The temperature about 2.5nm due to LaAlO substrate.

dependence of mechanics and electric coupling properties determined the phase properties of LaGdCoO and ZnO thin films. The phase-field of domain structure in epitaxial $\text{ZnO}/\text{La}_{0.4}\text{Gd}_{0.1}\text{Sr}_{0.5}\text{CoO}_3$ and gain size effect of our sample have been investigated.

2. EXPERIMENTS

In order to obtained an appropriate chemical composition for present study, the target $\text{La}_{0.4}\text{Gd}_{0.1}\text{Sr}_{0.5}\text{CoO}_3$ was prepared from the analytically pure oxides used proportion of La_2O_3 , Gd_2O_3 , Co_3O_4 and SrCO_3 by solid state reaction, after repeated grinding and sintering at 1250 °C for 24h for $\text{La}_{0.4}\text{Gd}_{0.1}\text{Sr}_{0.5}\text{CoO}_3$. The ZnO was sintering at 500°C for 48h by solid state reaction. The LGSCO and ZnO layers were successively deposited on the single-crystal LAO (100) substrate by pulse laser deposition. The multilayer thin films were annealed at 800°C with an oxygen pressure 6 Pa for 5h in order to get better epitaxial character and oxygen doped deposit. The structure of the target and the orientation of the deposited film were studied by XRD (Bruker D8 Advance XRD, 40KV, 40mA, smallest angular step 0.0001°). The sample of heterojunction thin film was placed in a JanisCCS-300 closed-circuit refrigerator cryostat (JanisCCS-300) over the range from 50 to 300 K. The magnetic field of 0.2 and 0.5 T was supplied by the electromagnet perpendicularly applied to heterostructure.

The MR and ρ -T in film was studied in a JanisCCS-300 over the range from 50 to 300 K at 0.2 and 0.5T, respectively. The topography of $\text{ZnO}/\text{La}_{0.4}\text{Gd}_{0.1}\text{Sr}_{0.5}\text{CoO}_3/\text{LAO}$ was measured though the AFM image. The AFM surface morphology and phase field image for $\text{ZnO}/\text{La}_{0.4}\text{Gd}_{0.1}\text{Sr}_{0.5}\text{CoO}_3/\text{LAO}$ and $\text{ZnO}/\text{La}_{0.4}\text{Gd}_{0.1}\text{Sr}_{0.5}\text{CoO}_3/\text{Si}$ were characterized by atomic force microscopy (AFM), respectively.

3. RESULTS AND DISCUSSION

FIG.1 a, b show the AFM phase field image of the surface morphology $\text{ZnO}/\text{La}_{0.4}\text{Gd}_{0.1}\text{Sr}_{0.5}\text{CoO}_3/\text{LAO}$. The bright region is hard phase, and the dark region is soft phase. The FIG. show the surface roughness for phase boundary between the ferromagnetic metallic(FM) $\text{ZnO}/\text{La}_{0.4}\text{Gd}_{0.1}\text{Sr}_{0.5}\text{CoO}_3/\text{Si}$ was 2nm and the surface and the charge-ordered insulating phase, where the quality is very well.AFM results were presented for phase separation effect is also enhanced. The $\text{ZnO}/\text{La}_{0.4}\text{Gd}_{0.1}\text{Sr}_{0.5}\text{CoO}_3/\text{LaAlO}$ and $\text{ZnO}/\text{La}_{0.4}\text{Gd}_{0.1}\text{Sr}_{0.5}\text{CoO}_3/\text{ZnO}$ junction exhibited excellent $\text{La}_{0.4}\text{Gd}_{0.1}\text{Sr}_{0.5}\text{CoO}_3/\text{Si}$,respectively.

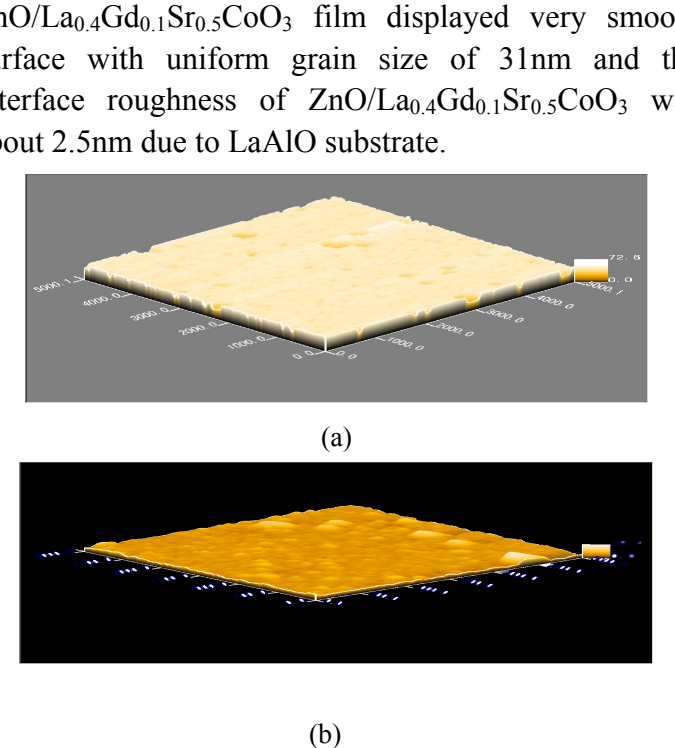
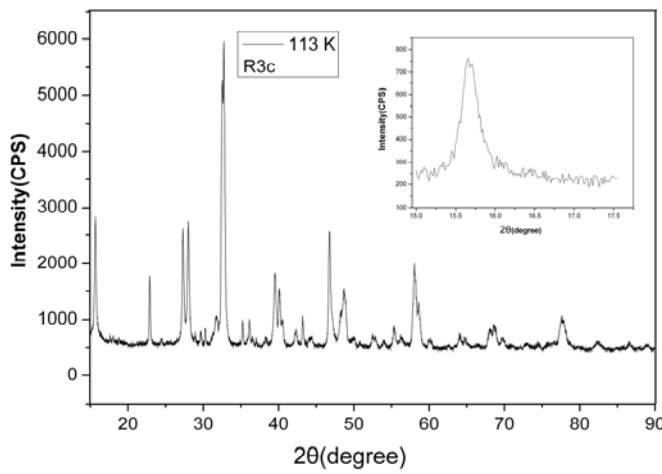
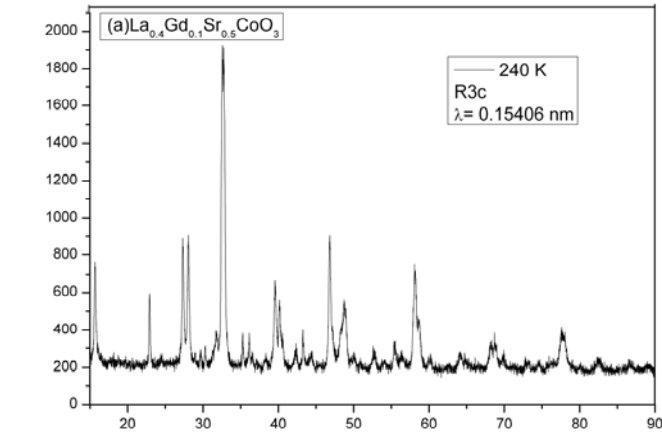


FIG.1. a. AFM phase field image of the surface morphology $\text{ZnO}/\text{La}_{0.4}\text{Gd}_{0.1}\text{Sr}_{0.5}\text{CoO}_3/\text{LAO}$. The bright region is hard phase, and the dark region is soft phase. FIG.1.b The AFM image of surface morphology $\text{ZnO}/\text{La}_{0.4}\text{Gd}_{0.1}\text{Sr}_{0.5}\text{CoO}_3/\text{LAO}$.

Fig.2 shows an evidences of two phase Rietveld refinement at 113 K($<\text{T}_{\text{CO}}$). These two perovskite phases can be characterized by the length of c, long c and short c respectively. The final refinement is satisfied with R3c group. We explored that the crystal symmetry group at room temperature is orthorhombic (Pbnm) without detected impurities. Fig.2(a) showed the sample of the Rietveld refinement at 240 K. Fig.2(b) indicated that the XRD are satisfactory, these two perovskite phases as result of single orthorhombically disordered perovskite (Pbnm;) and rhombohedral ($\bar{R}\bar{3}c$).

The LGSCO/ ZnO structure was characterized by x-ray diffraction pattern at 220K shown in Fig. 2. Two crystalline phases were identified from the XRD patterns. One was ZnO film crystalline phase of a hexagonal wurtzite. Other was LGSCO crystal phase of

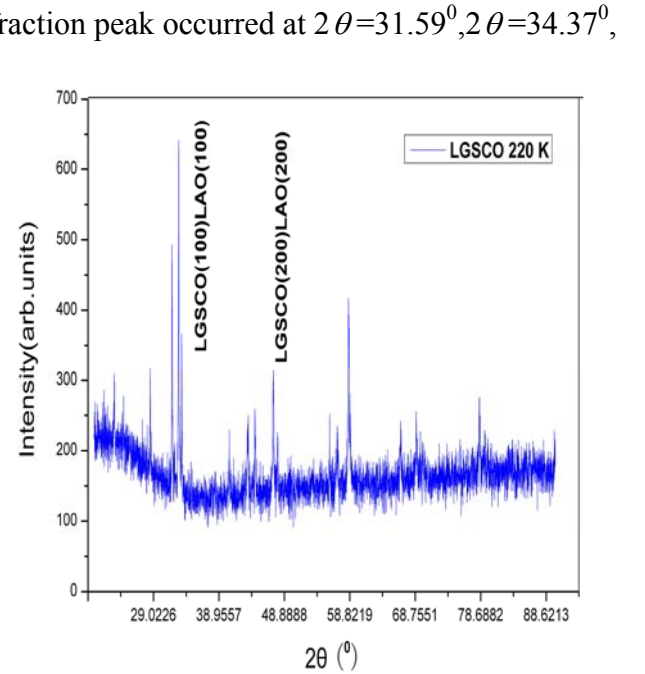
hexagonal perovskite structures (space group:R3c) with no more than 1% Co_3O_4 as the second phase by grain refinements.



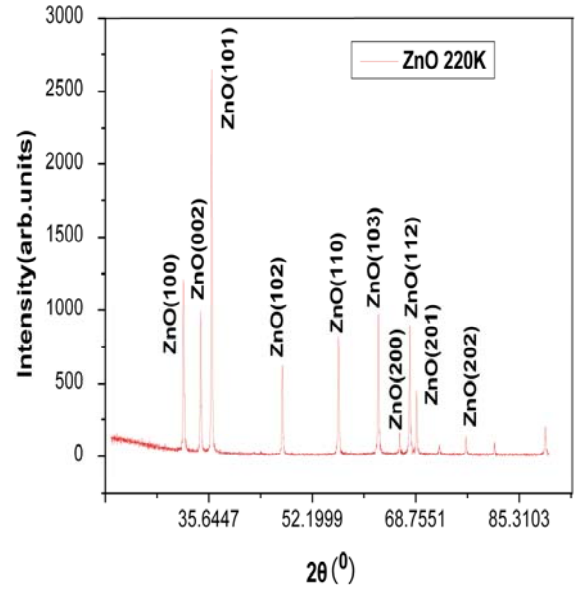
(b)

Fig.2 X-ray powder pattern for $\text{La}_{0.4}\text{Gd}_{0.1}\text{Sr}_{0.5}\text{CoO}_3$ (a) at 240 K and (b) at 113 K. Solid curve is the result of the Rietveld analysis with (a) single orthorhombically distorted perovskite (Pbnm;) phase from $\text{La}_{0.5}\text{Sr}_{0.5}\text{CoO}_3$ rhombohedral ($R\bar{3}c$) to $\text{Gd}_{0.5}\text{Sr}_{0.5}\text{CoO}_3$ orthorhombic (Pmmm), and with two perovskite phases, respectively.

It is known that the charge and orbital ordering transition at Gd half filling ($x \sim 0.5$) is strongly coupled with lattice distortion. The CoO_6 is distortion of oxygen octahedral. The LGSCO lattice parameters, Co-O bond length and Co-O-Co bond angle, were adjusted by Gd^{3+} ions size, and dependence on average radio of A (La, Gd) and site ion $\langle A \rangle$. The Fig.3(a) image indicated that the $\text{La}_{0.4}\text{Gd}_{0.1}\text{Sr}_{0.5}\text{CoO}_3$ (100) and (200) diffraction peaks occurred at $2\theta = 32.8^\circ$ and $2\theta = 47.2^\circ$, while the Fig.3(b) ZnO (100) (002) (101) (102) (110) (103) (200)



(a)



(b)

Fig.3 X-ray diffraction of $\text{ZnO}/\text{La}_{0.4}\text{Gd}_{0.1}\text{Sr}_{0.5}\text{CoO}_3/\text{LAO}$ heterostructure at 220K. The Figure (a) (b) shows the (100) and (200) peaks of the LGSCO film (a) and ZnO film (b).

$2\theta = 36.09^\circ$, $2\theta = 47.3^\circ$, $2\theta = 56.4^\circ$, $2\theta = 62.78^\circ$ and $2\theta = 66.15^\circ$. The spectrum peak showed crystal indices of LGSCO. The diffraction peaks of LAO (100), (200) substrate appear at $2\theta = 23^\circ$ and $2\theta = 47^\circ$. This chart identified LGSCO film in the crystal plane (100) identically matching with the LAO substrate with multi-crystal structure. The XRD of $\text{La}_{0.4}\text{Gd}_{0.1}\text{Sr}_{0.5}\text{CoO}_3$ has GdO characteristic diffraction peak at $2\theta = 28^\circ$. The doped Gd goes in to the LGSCO lattice. Because the Gd^{3+} electronic structure is $4f^7$, Gd^{3+} ion radius is

smaller than La^{3+} and Sr^{2+} . The Gd^{3+} has an effect on both structure factor and electronic state balance.

Table 1, structure and properties of $\text{La}_{0.5}\text{Sr}_{0.5}\text{CoO}_3$ and ZnO (\AA)

Ln	A	ZnO	Space group	$\langle r_A \rangle$	$\sigma(A^2) \langle A \rangle^0$	Lattice parameter (\AA)		
						a	b	c
La	Sr		R3c	1.400	0.0016	5.4152		
Gd	Sr		Pnma	1.329	0.0123	5.3746, 7.5601, 5.3723		
$\text{La}_{0.255}\text{Gd}_{0.245}\text{Sr}_{0.5}\text{CoO}_3$			R3ch	1.363	0.0081	5.3948		
$\text{La}_{0.4}\text{Gd}_{0.1}\text{Sr}_{0.5}\text{CoO}_3$			Pm3m	1.329	0.00468	3.8402		
ZnO			P63mc	1.99	0.0471	3.2511, , 5.1993		

We listed the weighted average radius given in peak, XRD wavelength, diffraction angle and Table 1.³⁰ The $\text{La}_{0.5}\text{Sr}_{0.5}\text{CoO}_3$ have representative 12 proportional constant K, we calculated the average coordination number of A sited cations, as well as grain size of LaGdSrCoO_3 film using the Scherrer $\text{Gd}_{0.5}\text{Sr}_{0.5}\text{CoO}_3$ representative 9. The structure exhibit equation. The LaGdSrCoO_3 average grain size of the that when A=Sr, the LnACoO_3 structure is film was 30.7 nm in coincidence with AFM results.

rhombohedral (space group: $\bar{R}\bar{3}c$) until $\text{Ln} = \text{La}$. The Sr-site coordination number is 12 when the crystal structure is rhombohedral, and 9 when it is orthorhombic. In the situation of A=Sr, $\text{Ln}=\text{La}$, Gd, we could get an satisfactory good fit for the Pnma,

Pm3m and $\bar{R}\bar{3}c$ space groups, and we have, furthermore, preferred the space group with higher symmetry as per the normal practice. The rhombohedral and orthorhombic structure illustrate how the CoO_6 octahedra is distorted in the orthorhombic structure, especially in $\bar{R}\bar{3}c$ and Pm3m space group of the $\text{La}_{0.4}\text{Gd}_{0.1}\text{Sr}_{0.5}\text{CoO}_3$. The Co-O bond increase with the variation from $\text{La}_{0.5}\text{Sr}_{0.5}\text{CoO}_3$ to $\text{La}_{0.4}\text{Gd}_{0.1}\text{Sr}_{0.5}\text{CoO}_3$, at the same time the Co-O bond decrease.

The antiferromagnetic spin-ordering accompanied is for the long c phase. To determine critical a charge-order transition with CO phase structure temperature, i.e., Curie temperature T_c and the exhibited a strong correlated coupling between the charge-ordering temperature T_{co} , we have tested spin and orbital degrees of freedom. The diffraction temperature dependence of resistivity and peak of $\text{ZnO}/\text{La}_{0.4}\text{Gd}_{0.1}\text{Sr}_{0.5}\text{CoO}_3$ was matched with magnetization. The resistance decrease with an the LAO substrate (lattice constant 0.38769 nm) when the lattice constant was 0.386 and 0.379nm respectively. The results indicated that the $\text{La}_{0.4}\text{Gd}_{0.1}\text{Sr}_{0.5}\text{CoO}_3$ and ZnO thin films had better epitaxial characters respectively. The ZnO film is separated behavior(two phase). T_c is determined $2\theta=34^0$ for the (002) orientation with the structure of from the R-1/T curve, which measured an IM a hexagonal wurtzite. According to the width of half transition at 128 K. The T_c goes up to a $\langle r_A \rangle$ value of increase of temperature, $1.45 \times 10^6 \Omega$ for 100K and $5.81 \times 10^5 \Omega$ for 280K, exhibits a LGSCO phase

(1). Electronic feature of phase separated state

Figure 4, we showed the temperature dependence of the ZnO/LGSCO junction resistance, and Figure 5 MR of compositions of LGSCO at variation 0.2T, 0.5T. The magnetoresistance mechanism in perovskite cobalt oxides attracted special interested due to its T_c sensitivity and cation-size mismatch applications. The most important message of Fig.2 is that domain boundary and lattice mismatch. The lattice constant shows a discontinuous change at T_{co} . In another word, the system is transformed into phase separation. Such a paramagnetic state at T_{co} 200 K is described to the random nucleation of a low temperature phase and subsequent stress-induced growth of the secondary phase. The phase separation is considered stress-induced phase separation which is origin from lattice constant. At T_{co} 200 K, a b and the short c is for paramagnetic insulator while those ferromagnetic

LGSCO and decease therefore. The resistance of cobaltates also increases with the effects of cation size and mismatch disorder. This result also show the effect of carriers captured at interface. Both $\text{La}_{0.4}\text{Gd}_{0.1}\text{Sr}_{0.5}\text{CoO}_3$ and ZnO show the expected metallic behavior, but orthorhombic $\text{Gd}_{0.5}\text{Sr}_{0.5}\text{CoO}_3$ show a slight departure from metallic behavior. While $\text{La}_{0.4}\text{Gd}_{0.1}\text{Sr}_{0.5}\text{CoO}_3$ at low temperature is metallic, $\text{La}_{0.4}\text{Gd}_{0.1}\text{Sr}_{0.5}\text{CoO}_3$ at high temperature is an insulator.

(2) Magnetic feature of phase separated state

The experiment shows important role of cation size and disorder on both the electric and the magnetic resistance properties. A large lattice mismatch led to more defects at interface, and captured more carriers.

The lower the temperature, the more carriers will be captured, and the junction resistance is increased. On the other hand, the electrons transport and M-I transition based on double exchange and polarons hopping were due to spin-orbit coupling between localized electrons Co-3d t_{2g} and itinerant electrons O-2p e_g in the films. With an increase of temperature above T_{co} , the sample properties represent the intensity characteristics to the single glass phase and COI insulator, because the charge-orbital ordering transition. With a decrease of temperature below T_{c} shown as Fig5 (a) behaviour of $\text{Log } \rho$ versus T for the LGSCO/ZnO (b) behaviour of ρ/T versus $1/T$ for the LGSCO/ZnO, the components represent the intensity properties to two phases, ferromagnetic and anti ferromagnetic ordering, because long c lattice constant is for spin transition. Such state is described to the strong coupling system between the orbital and lattice degree of freedom via the Jahn-Teller effect. The magnetoresistance is defined as $\text{MR} = \Delta R/R = (R_H - R_0)/R_0$ where R_H is the resistance of heterojunction with the applied magnetic field, R_0 is the resistance without the magnetic field shown in Fig.5c. The temperature was dependence of junction $\Delta R/R$ and MR of the heterostructure. We could measure the charge-orbit variation and spin-orbital coupling from junction $\Delta R/R$ and MR. Here, we have exhibited lattice constant C for the magnetic feature: short c is for ferromagnetic and antiferromagnetic type, further short c for COI. As well as, we described the long c for ferromagnetic and

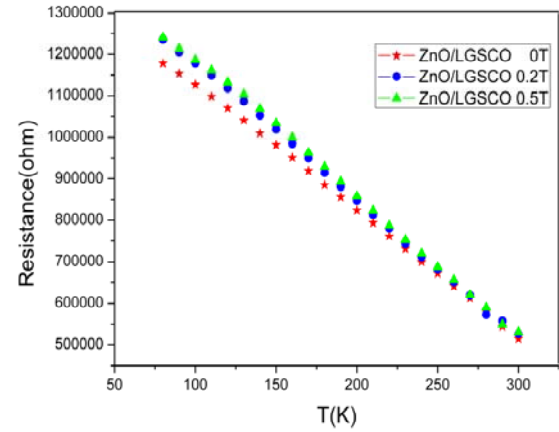
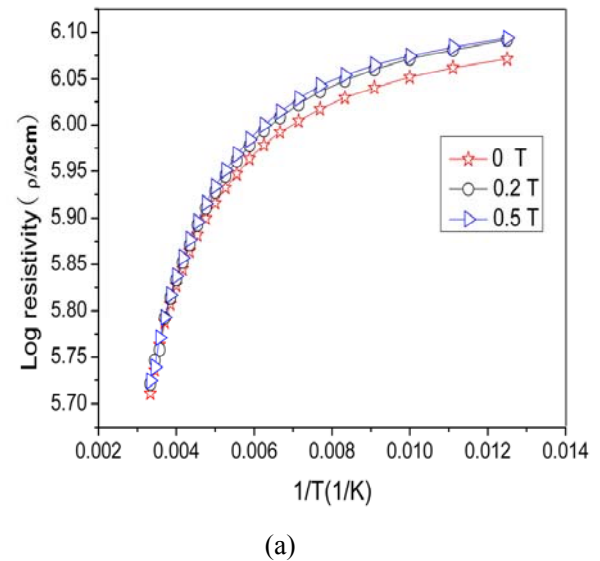
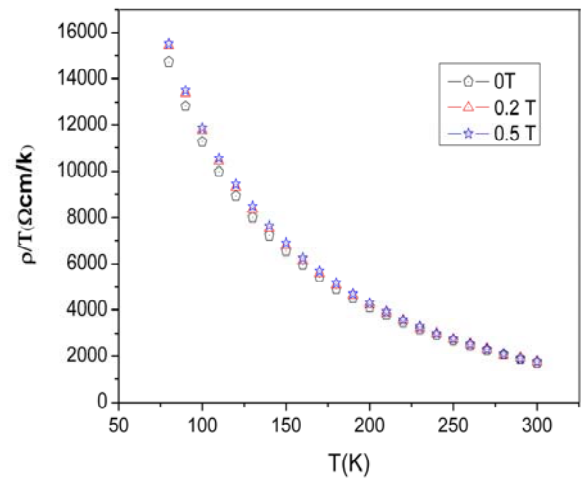


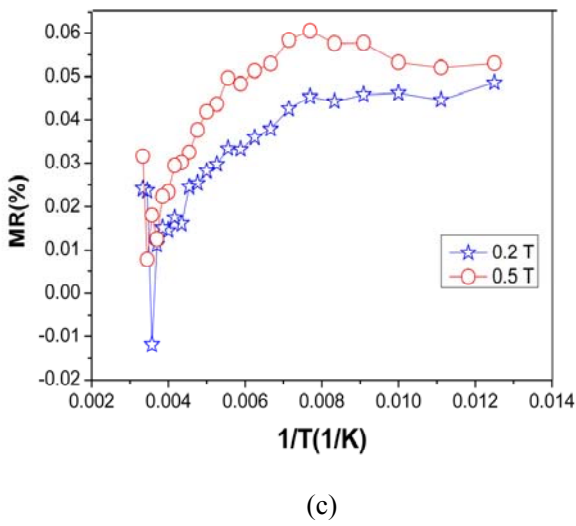
Fig4. Temperature dependence of LGSCO/ZnO junction resistance of the heterostructure under applied different magnetic field.



(a)



(b)



(c)

Fig5. (a) Behaviour of $\log \rho$ versus T for the LGSCO/ZnO (b) including Landau, gradient, electrostatic and elastic energies.

(c) Temperature dependence of the LGSCO/ZnO junction magnetic resistance at magnetic field $H = 0.2$ and 0.5 T.

Our observation clearly demonstrates that the magnetic domain structures in LGSCO vary significantly with the doping level.^{7,8,24-27} The antiferromagnetic spin. The LGSCO MR had MIT polarizations within these two doping level variants properties and exhibited a steep increase in the are related to 71^0 and 109^0 domain walls. The domain LGSCO single layer structure at the low temperature. are oriented along (100) or (010) directions of the Over the range of temperature less than 130 K, the substrate. The red and yellow are typically paired. junction displayed a metallic-like in which there was temperature dependence of $d(MR)/dT > 0$. Coexisting shown in Fig. 6, the domain splits into several parts. of the ferromagnetic and antiferromagnetic ordering When the sample was warming up above T_c , and the could be concluded to a canting spin structure, such sample was cooled from above T_c to lower the case of the double layer manganites temperature, the properties of domain appear. The $\text{La}_{2-2x}\text{Sr}_{1+2x}\text{Mn}_2\text{O}_7$. Actually, the ρ - T curve at $y=0.5$ domain stared to appear at medium temperature. The Co shows a significant I-M behavior at around domain structure of polycrystalline LGSCO thin film $T_c=127$ K.^[1-19,21-26]

Moreover, domain structure takes effect on the boundary resistivity of LGSCO film, finally varied the charge-ordering temperature and Curie temperature, ferromagnetic metal to paramagnetic insulator respectively. COI above TCO stand for occurred at Curie temperature T_c 127 K. The charge-ordering insulator, thus, PI and FM stand for maximum value of the positive MR at 0.2 T is 4.86%, the paramagnetic insulator and ferromagnetic metallic at 0.5 T is 6.05% for approximately 140K. There were phase at T_c . domain wall orientations and domain main factors which influenced the spin orientation of structure strongly influence the paramagnetic insulator Co^{3+} and Co^{4+} .^{15,28,29,30} We speculated that the junction properties of LGSCO, furthermore, change the resistance was mostly derived from the interface junction properties at LGSCO/ZnO thin film.

The phase field dynamics was adopted to explore between ZnO and LGSCO which the junction possibilities of substrate effect and external field on resistance in ZnO and LGSCO films was altered by the lattice. The anisotropy caused by changes of the ZnO/LGSCO interfacial phase cluster, bond length substrate stress and magnetic field, is enough to and the band angle of Co^{3+} -O- Co^{4+} chain. Thus, the produce observation area of domain structure change. carrier transfer of heterjunction was derived from the

We adopted the two rectangular systems, one is local system which the pseudocubic crystal cell, other is globe system with orthogonal axes x_i , x_i and x_i in the film plane.

We begin the simulation with small random polarization. The P_3 polarization component was built by the magnetic field and voltage resulting from the film/substrate interface. The evolution of phase field of polarization is controlled by the time-dependent Ginzburg-landau and Cahn-Hilliard free energy equation.^{13,14}, $\frac{\partial P_i(r,t)}{\partial t} = -L \frac{\delta F}{\delta P_i(r,t)}$ ($i = 1,2,3$), Where L is

the kinetic coefficient, and the L is related with domain wall mobility. F is the total free energy

Our observation clearly demonstrates that the magnetic domain structures in LGSCO vary significantly with the doping level.^{7,8,24-27} The

We obtain the ferroelectronic phase image of the spontaneous polarization process (The number of iterations step $t=3000-5000$) was shown in Fig 6. Further, the phase transition of junction from charge-ordering insulator and ferromagnetic metal to paramagnetic insulator respectively. COI above TCO stand for occurred at Curie temperature T_c 127 K. The charge-ordering insulator, thus, PI and FM stand for maximum value of the positive MR at 0.2 T is 4.86%, the paramagnetic insulator and ferromagnetic metallic at 0.5 T is 6.05% for approximately 140K. There were phase at T_c . domain wall orientations and domain main factors which influenced the spin orientation of structure strongly influence the paramagnetic insulator Co^{3+} and Co^{4+} .^{15,28,29,30} We speculated that the junction properties of LGSCO, furthermore, change the resistance was mostly derived from the interface junction properties at LGSCO/ZnO thin film.

diffusion of ZnO/LGSCO due to the lattice mismatch

domain boundary scattering and capture effect, which were controlled by optical and magnetic perturbations.

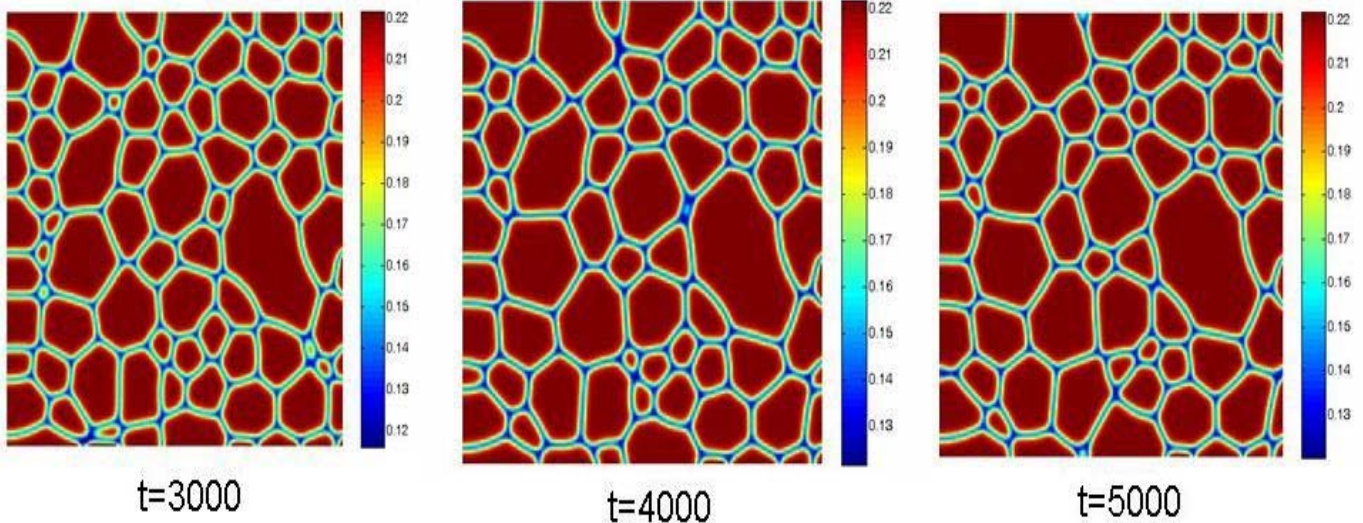


Fig.6. The domain structure of polycrystalline LGSCO thin film of the spontaneous polarization process (The number of iterations step $t=3000-5000$)

4. CONCLUSIONS

In summary, the presence of FM phase and carrier Nonequilibrium of China 2009 (Grant No. 2009, injection effect mechanism is clearly demonstrated in 1001).

the $\text{ZnO}/\text{La}_{0.4}\text{Gd}_{0.1}\text{Sr}_{0.5}\text{CoO}_3$. The ferromagnetic **REFERENCES**

ACKNOWLEDGEMENTS

This work is supported by MOE Key Laboratory for

- [1] J.B Goodenough, Phy,Rev.100, 564(1955)
- [2] R.Lengsdort, M. Ait-Tahar,S.S.Saxena et al, Phys. Rev. B. 69, 140403, (2004)
- [3] R.Vonhelnolt, J. Wecker, B.Holzapfel, L.Schultz, K. Samwer, Phys.Rev.Lett. 71,2331(1993)
- [4] N. A. Spaldin and M. Fiebig, Science 309, 391 (2005).
- [5] C. Zener, Phys.Rev. 82,403(1951)
- [6] M.M. Savosta, P.Novak,Phys.Rev.Lett.87,137204
- [7] A Machida, T.Watanuki,D.Kawana, Physical Rev. B, 83(5), 054103,(2011).
- [8] S. Jin, T. H. Tiefel, M. McCormack, R. A. Fastnacht, R. Ramesh, and L.H. Chen, Science 264, 413 (1994)
- [9] S Mori, R Shoji, N Yamamoto, T Asaka, Y Matsui, Y Moritomo, Physical Rev. B, 67(1), 012403,(2003).
- [10]Clément Barraud, Pierre Seneor, Richard Mattana, Stéphane Fusil, Karim Bouzehouane, Cyrille Deranlot, Patrizio Graziosi, Luis Hueso, Ilaria Bergenti, Valentin Dedi, Frédéric Petroff & Albert Fert, Nature Physics 6, 615-620(2010)
- [11]T. Botond,C. Ioan-Augustin,N. Zoltan,Central European Journal of Physics,11(4), 487-496

(2013).

[12] S. H. Baek, H. W. Jang, C. M. Folkman, Y. L. Li, B. Winchester, J. X Zhang, Q. He, Y. H. Chu, C. T. Nelson, M. S. Rzchowski, X. Q. Pan, R. Ramesh, L. Q. Chen, and C. B. Eom, *Nature Mater.* 9, 309 (2010).

[13] W. Luo, F. Shi, F. Wang, *J. Magnetism and Magnetic Material*, 305, 509(2006)

[14] J. Wang, J. B. Neaton, H. Zheng, V. Nagarajan, S. B. Ogale, B. Liu, D. Viehland, V. Vaithyanathan, D. G. Schlom, U. V. Waghmare, N. A. Spaldin, K. M. Rabe, M. Wuttig, and R. Ramesh, *Science* 299, 1719 (2003)

[15] J. X. Zhang, Y. L. Li, S. Choudhury, L. Q. Chen, Y. H. Chu, F. Zavaliche, M. P. Cruz, R. Ramesh, and Q. X. Jia, *J. Appl. Phys.* 103, 094111 (2008).

[16] F. Fan, CL Chen, BC Luo, J. Appl. Phys. 109, 073716, (2011)

[17] J. Wu, X. Lou, Y. Wang, and J. Wang, *Electrochem. Solid-State Lett.* 13, 2 (2010)

[18] JB Goodenough, F Rivadulla, E Winkler, *Central Europhysics Letters*, 61(4), 527 (2003)

[19] G. Gutierrez and M. J. Yacaman, *J. Phys. Chem. B* 109, 3813 (2005).

[20] JB Goodenough, RI Dass, *International Journal of Inorganic Materials*, 2, 3-9(2000)

[21] C. Mitra, P. Raychaudhuri, K. Dörr, K. H. Muller, L. Schultz, P. M. Oppeneer, and S. Wirth, *Phys. Rev. Lett.* 90, 017202(2003)

[22] Mariscal, M. M.; Velazquez-Salazar, J. Jesus; Yacaman, M.J., *CrystEngComm*, 14, 544-549 (2012)

[23] GC Xiong, B Zhang, SC Wu, ZX Lu, JF Kang, GJ Lian, DS Dai, *Solid State Comm.* 97, 17 (1996)

[24] W. Yang, Y. Chang, C. Huang, Y. Chen, *J. Electronic Materials* 38(3), 460(2009)

[25] G. Yuri I, K. Volodymyr V., *Central European Journal of Physics*, 11(3), 375, (2013)

[26] J. Wu, C. Leighton, *Phys. Rev. B* 67, 174408(2003)

[27] M.G. Aleksandra, L. Tomasz, G.K. Katarzyna, *Central European Journal of Physics*, 11(2), 213, (2013)